Magnetic structure of relativistic systems with low symmetry

L. M. Sandratskii
Institut für Festkörperphysik, Technische Universität, 64289 Darmstadt, Germany
(Received 2 April 2001; published 28 August 2001)

The notion of symmetry constraint is used to discuss the stability of the regular features of magnetic structures in the density-functional theory (DFT) calculations and in nature. On the basis of symmetry arguments and first-principles DFT calculations it is shown that the magnetic structure of a relativistic system with atomic disorder is always noncollinear. The symmetry analysis and illustrative first-principles DFT calculations for a series of magnetic configurations relevant to the magnetism of rare-earth metals are reported and used to discuss the role of the spin-orbit coupling in the formation of the magnetic structure in these systems.

DOI: 10.1103/PhysRevB.64.134402 PACS number(s): 75.25.+z, 71.15.Mb, 71.70.Ej, 75.10.Lp

I. INTRODUCTION

The relation between the symmetry and magnetic structure of a system attracted much attention in the history of solid-state magnetism. Much consideration was given to the prediction of the magnetic structures that can appear in the system as result of a continuous phase transition (see, e.g., Refs. 1 and 2).

The subject of the present discussion is different. It is the stability of a given magnetic configuration, independent of the kind of the phase transition into magnetic state. The interest to this problem is strongly stimulated by recent developments in the density functional theory (DFT) that made possible first-principles calculation of complex noncollinear magnetic configurations (see, e.g., Ref. 3 for review). These calculations have shown that the magnetic structure chosen at the beginning of the DFT calculation is, in general, unstable: the magnetic moments deviate in the course of iterations from the initial directions tending to form another magnetic state. On the other hand, in some cases the magnetic moments, although allowed to move, keep their initial directions. The ability to predict to which of the two types of structures a given magnetic configuration belongs is an important help in the study of the magnetism of the system.

In previous work[4–6] we have shown that there exists an intimate connection between the stability of the magnetic structure in the DFT calculations and the symmetry of the system. A criterion was formulated that allows the prediction of the instability of a given magnetic configuration on the basis of the symmetry analysis. Applications of the criterion to cardinally different magnetic systems have been reported. For example, it was shown that in U_3P_4 the collinear magnetic structure cannot be stable.[4] This instability is a consequence of symmetry properties and relativistic interactions. In UFe_4Al_8, the criterion was used to explain an unusual relative orientation of the magnetic moments of the Fe and U sublattices.[5] In UPtGe, the symmetry arguments helped to understand the unique helical structure of this system.[6]

The aim of the present paper is twofold. In the first part, we use the notion of symmetry constraint to give a solid mathematical basis to the symmetry treatment. We extend the discussion of the stability of a magnetic structure to the stability of particular regular features of the magnetic configuration. In the second part, a number of applications of the symmetry approach to interesting magnetic systems is reported. The symmetry analysis is combined with first-principles DFT calculations.

Note, that a close connection between the symmetry of the Hamiltonian of the problem, on the one hand, and the properties of the theoretical magnetic ground state, on the other hand, is a common feature of all theoretical models (see, e.g., an early paper by Lyons and Kaplan[7] on the properties of the Heisenberg model of classical atomic spins as an example). Depending on approximations used in the formulation of the theoretical model, the symmetry of the Hamiltonian can substantially vary, even in the consideration of the same physical system. In an ideal case, these approximations reflect the hierarchy of the interactions in the system and provide a desired accuracy of the description of the properties studied.[8] The following features characteristic for the DFT are important for the present discussion. First, in the DFT there is no separate equation for the magnetic degrees of freedom. The equations of the theory are formulated for the spinor wave functions of the effective electron states. The effective potential entering the equation depends on the charge and magnetization densities and is considered in its full-space dependence. The magnetization of the system appears as a sum of the magnetic polarizations of the individual electron states. Such an approach limits drastically the possibility of approximations in the physical model that influence the symmetry of the problem. Different DFT schemes vary mainly in the form of the exchange-correlation potential and in the method of the numerical solving of the Kohn-Sham equation, both do not change the symmetry of the Kohn-Sham Hamiltonian (KSH). There is, however, an important difference in the symmetry of relativistic and nonrelativistic KSH.[3] The consequences of this difference are an important part of the present discussion.

Second characteristic feature of the DFT is also related to the complexity of the calculational task and consists in the iterational method of solving the problem. As we will show, the iterational procedure of the DFT is subjected to the symmetry constraint. Analysis of the properties of the symmetry constraint is useful in the studies of the stability of regular features of magnetic structures.

II. SYMMETRY CONSTRAINT

A. General formulation

We begin with the proof of the statement that the symmetry of the initial Kohn-Sham Hamiltonian is preserved in the iterational DFT calculations. Let us assume that the initial KSH of the problem commutes with the operators of group G and show that the density matrix, obtained with the use of the solutions of the Kohn-Sham equation, is invariant with respect to the operators of G. The concrete form of the KSH is not important here. (See, e.g., Refs. 9 and 3 for the description of the KSH of a noncollinear relativistic magnet.) For nonrelativistic problems the operations are of the $\{\alpha_S|\alpha_R|\mathbf{t}\}$ type where α_S is a spin rotation, α_R is a space rotation, $\mathbf{t}$ is a space translation.[3] In the case of relativistic problems α_S is always equal to α_R and the operators are of the $\{\alpha_R|\alpha_R|\mathbf{t}\}\equiv\{\alpha_R|\mathbf{t}\}$ type.[3] In both cases these transformations can be accompanied by the time reversal.

The density matrix of the system can be written in the form

$$\rho(\mathbf{r})=\sum_{i,occ}\psi_i(\mathbf{r})\psi_i^{\dagger}(\mathbf{r}), \tag{2.1}$$

where ψ are the two-component eigenspinors of the KSH; the sum runs over occupied states.

According to the basic theorems of quantum mechanics, if operator $\hat{g}$ commutes with Hamiltonian $\hat{H}$ and ψ is an eigenfunction of $\hat{H}$ corresponding to eigenvalue ε, then $\hat{g}\psi$ is also an eigenfunction corresponding to the same energy. As a consequence, all eigenstates of $\hat{H}$ can be separated into the subsets such that the states of one subset correspond to the same energy and form a basis of an irreducible representation of G. The contribution to the density matrix of any such subset is invariant with respect to the operations of G. Indeed,

$$\begin{aligned}
&\hat{g}\sum_{\nu}\psi_{\nu}^{j}(\mathbf{r})\psi_{\nu}^{j\dagger}(\mathbf{r})\\
&=\sum_{\nu}\hat{g}\psi_{\nu}^{j}(\mathbf{r})[\hat{g}\psi_{\nu}^{j}(\mathbf{r})]^{\dagger}\\
&=\sum_{\nu}\sum_{\mu}D_{\mu\nu}^{j}(\hat{g})\psi_{\mu}^{j}(\mathbf{r})\left[\sum_{\eta}D_{\eta\nu}^{j*}(\hat{g})\psi_{\eta}^{j}(\mathbf{r})\right]\\
&=\sum_{\mu\eta}\left[\sum_{\nu}D_{\mu\nu}^{j}(\hat{g})D_{\eta\nu}^{j*}(\hat{g})\right]\psi_{\mu}^{j}\psi_{\eta}^{j}\\
&=\sum_{\nu}\psi_{\nu}^{j}(\mathbf{r})\psi_{\nu}^{j\dagger}(\mathbf{r})
\end{aligned} \tag{2.2}$$

Here D^j is the jth irreducible representation of G.

Since

$$\rho(\mathbf{r})=\frac{1}{2}\begin{pmatrix} n(\mathbf{r})+m_z(\mathbf{r}) & -im_x(\mathbf{r})+m_y(\mathbf{r})\\ im_x(\mathbf{r})+m_y(\mathbf{r}) & n(\mathbf{r})-m_z(\mathbf{r})\end{pmatrix}, \tag{2.3}$$

the invariance of the $\boldsymbol{\rho}$ matrix immediately means the invariance of the particle density n and spin magnetic density $\mathbf{m}$ with respect to $\hat{g}$. Therefore the effective potential

$$\boldsymbol{v}(\mathbf{r})=v_{\bigcirc}[n(\mathbf{r})]+\Delta v[n(\mathbf{r}),\boldsymbol{m}(\mathbf{r})]\boldsymbol{\sigma}\cdot\frac{\boldsymbol{m}(\mathbf{r})}{|\boldsymbol{m}(\mathbf{r})|} \tag{2.4}$$

calculated with the use of densities n and $\mathbf{m}$ is also invariant with respect to $\hat{g}$. As a result, the KSH for the next iteration, which uses the calculated effective potential (2.4), is again, as the initial one, invariant with respect to operations of G.

Thus we have shown that the densities obtained in the calculations are invariant with respect to the symmetry operations of the initial KSH and any symmetry operation of the initial KSH is preserved in the calculations. Since only the densities invariant with respect to operations of G appear in the calculations, one deals with a constrained minimization of the total energy considered as a functional of the densities. We will refer to this type of restrictions on the densities as symmetry constraint.

A general approach to a constrained minimization of the energy as a functional[10,11] of the charge and magnetic densities requires adding to the functional the following term:

$$\int d\mathbf{r}p(\mathbf{r})[\hat{g}n(\mathbf{r})-n(\mathbf{r})]+\mathbf{b}(\mathbf{r})[\hat{g}\mathbf{m}(\mathbf{r})-\mathbf{m}(\mathbf{r})].$$

This term contains Lagrange parameters $p(\mathbf{r})$ and $\mathbf{b}(\mathbf{r})$ that play the role of external fields stabilizing the constrained state.

A remarkable feature of the symmetry constraint is that the state providing the minimum of the functional under the symmetry restriction does not need a nonzero stabilizing external field. This follows from the property that the symmetry of the KSH and densities is preserved in calculations.[12]

The property that a symmetry-constrained state does not need an external stabilizing field is of exceptional importance since only such states can be the ground state of the system. This property permits cardinal simplification of the calculation of the ground state if the experimental data and theoretical considerations evidence the presence of certain symmetry in the system. Note, that the DFT allows, in principle, to begin calculations with a random magnetization and, by carrying out the iterational process to self-consistency, to determine the magnetic state with the minimal energy. A highly symmetrical ground state can be established in such calculations since, opposite to the loss of symmetry, an increase of symmetry in the DFT calculations is possible. These calculations are, however, extremely complex and time consuming even for the simplest magnetic systems. Therefore, the symmetry constraint is an efficient tool in the DFT studies of magnetic systems.

B. Two types of symmetry constraints

We will distinguish two types of symmetry constraints. To introduce them we consider in more detail the restrictions imposed on the magnetization by the condition that the magnetization is invariant with respect to the operations of group G.

Since, on the one hand, the symmetry operation $\hat{g}$ transforms the magnetic density $\boldsymbol{m}(\mathbf{r})$ and, on the other hand, leaves it invariant, the magnetization must fulfill the following condition[13]

$$\{\alpha_S|\alpha_R|\mathbf{t}\}\mathbf{m}(\mathbf{r})\equiv\alpha_S\mathbf{m}(\{\alpha_R|\mathbf{t}\}^{-1}\mathbf{r})=\mathbf{m}(\mathbf{r}) \qquad (2.5)$$

After integration of the magnetization over atomic spheres we get the restriction

$$\mathbf{m}_i=\alpha_S\mathbf{m}_j \qquad (2.6)$$

imposed on the atomic magnetic moments where i and j label the atoms defined by the relation

$$\{\alpha_R|\mathbf{t}\}\mathbf{a}_i=\mathbf{a}_j\,. \qquad (2.7)$$

Therefore the atoms that are transformed one into another by $\hat{g}$ possess the magnetic moments of equal magnitude, and the direction of one moment is transformed into the direction of another under the action of $\hat{g}$. In the case the position of an atom is unchanged under the action of $\hat{g}$, Eq. (2.6) takes the form

$$\mathbf{m}_i=\alpha_S\mathbf{m}_i$$

and imposes a restriction on the moment of this atom that consists in the invariance of the moment with respect to $\hat{g}$. If operation $\hat{g}$ contains time reversal Eq. (2.6) is modified as follows:

$$\mathbf{m}_i=-\alpha_S\mathbf{m}_j\,. \qquad (2.8)$$

The restrictions (2.6)–(2.8) on the lengths and directions of the atomic magnetic moments can be considered as regular features (regularities) of the magnetic structure that are the necessary consequences of a given symmetry constraint. Two different situations can follow from relations (2.6)–(2.8). In the first case, the symmetry constraint determines the magnetic structure uniquely. This means that any deviation of the magnetic moments from the initial directions disturbs, at least, one of the symmetry operations. Since all symmetry operations must be preserved the structure cannot change in the course of calculations. We will refer to this type of constraint as symmetry constraint I. An example of symmetry constraint I is, e.g., the triple-**k** magnetic structure.[14]

In the second case (symmetry constraint II) there is an infinite set of magnetic configurations that, first, satisfy the conditions (2.6)–(2.8) imposed by the invariance with respect to G and, second, can be continuously transformed into one another without disturbing the symmetry of the system. Let θ be a continuous parameter that describes this set of magnetic configurations. (The number of parameters can be larger than one, but this does not change the essence of arguments.) As all magnetic configurations are described by the same symmetry none of the θ values is distinguished. The purpose of the DFT calculations in this case is to find the value of θ that corresponds to the state with the lowest energy. Since all θ values are equivalent, this minimum cannot be predicted without calculations (Fig. 1).

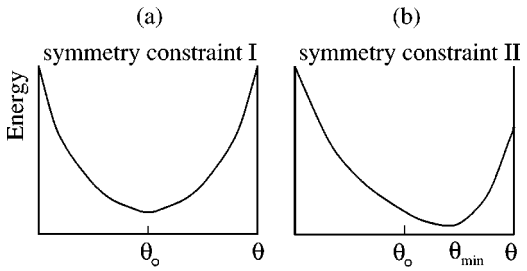

FIG. 1. Difference between symmetry constraints I and II (schematic picture). Continuous parameter θ describes different magnetic configurations. (a) The state with $\theta=\theta_{\bigcirc}$ corresponds to the symmetry constraint I. This state possesses additional regular feature compared with the states with $\theta\neq\theta_{\bigcirc}$ (b) Symmetry constraint II. The states with different θ possess the same regular features. Probability that $\theta_{\bigcirc}$ accidentally coincides with θ_{min} is negligible.

To begin the DFT calculation a value $\theta_{\bigcirc}$ of parameter θ is selected. Since it is improbable that $\theta_{\bigcirc}$ accidentally equals θ_{min} providing the minimum of the total energy the initial state in the case of symmetry constraint II is unstable. In the iterational process, the magnetic structure deviates from the state described by $\theta_{\bigcirc}$ tending to assume the state with the lowest energy. Note, that a self-consistent DFT calculation for the state with arbitrary θ is possible. Such calculations need, however, an additional (nonsymmetry) constraint on the system.[10] This additional constraint requires application of an external stabilizing field. Constrained calculations are a useful tool in studies of low-lying excitations.

The situation described by symmetry constraint II is related to many interesting physical phenomena. In a typical case the neglect of a part of interactions leads to the ground state of the system that belongs to constraint I and, therefore is uniquely determined by symmetry. With account for the full Hamiltonian this state corresponds, however, to symmetry constraint II. Therefore in the full-Hamiltonian study it becomes unstable and a variation of the state must take place. Examples of such systems are, e.g., Fe_2O_3 and Mn_3Sn where the spin-orbit coupling (SOC) leads to the phenomenon of weak ferromagnetism.[3]

Summarizing this section we can formulate a number of conclusions. First, a given magnetic structure is stable in the DFT calculations only in the case it corresponds to symmetry constraint I. Second, if the structure corresponds to symmetry constraint II its variation is subjected to restrictions imposed by the relations (2.6)–(2.8). Thus, although the structure itself is unstable, the regularities in the magnetic state that follow from Eqs. (2.6)–(2.8) are preserved features of the magnetic structure. On the other hand, an assumed regularity in the initial magnetic structure that is not supported by a symmetry operation is not a stable feature of the magnetic state of the system.

It is important to distinguish between the stability in the DFT calculations and the stability in the nature. Magnetic configurations stable in the calculations may not necessarily be the physical ground state, since random fluctuations characteristic of real systems are absent in the DFT calculations. Therefore the symmetry constraint is not efficient in the real systems. On the other hand, the instability of a magnetic

TABLE I. Noncollinear magnetic structure of distorted bcc iron: self-consistent relativistic calculations. Atomic positions and shifts are given in the units of the bcc lattice parameter, the deviation angles in degrees. Calculation 1 is performed for the atomic shifts given in the second column and unscaled SOC. Calculation 2 is performed for the SOC twice the normal value. In calculation 3 all atomic shifts are twice those given in the second column.

		Deviation of atomic moments			
		Calculation 1		Calculation 2	Calculation 3
bcc position	Shift	Spin θ,ϕ	Orbital θ,ϕ	Spin θ,ϕ	Spin θ,ϕ
(0,0,0)		0.81,188.8	1.63,215.6	1.15,165.0	0.82,184.9
$(\frac{1}{2},\frac{1}{2},\frac{1}{2})$	(0.01,0.02,0.03)	0.79,193.6	0.96,206.8	1.09,169.6	0.88,190.5
(0,0,1)	(0,0.01,0.01)	0.69,191.1	0.28,78.7	0.98,160.2	0.65,194.1
$(\frac{1}{2},\frac{1}{2},\frac{3}{2})$	$(-0.02,0,-0.01)$	0.73,188.8	1.26,309.2	1.06,160.1	0.69,187.5
(0,1,0)	$(0,-0.03,0)$	0.83,193.2	1.37,180.4	1.14,171.2	0.95,199.0
$(\frac{1}{2},\frac{3}{2},\frac{1}{2})$		0.81,194.5	1.48,233.8	1.08,173.0	0.90,205.1
(0,1,1)		0.72,195.4	0.93,78.4	0.96,168.3	0.82,209.0
$(\frac{1}{2},\frac{3}{2},\frac{3}{2})$		0.77,189.6	1.04,325.8	1.09,163.4	0.81,194.1

state in the DFT calculations can be directly related to the instability in nature, because this instability is a consequence of the interactions in the system. The latter property is of primary importance for the discussion of concrete physical systems in the following section.

III. APPLICATIONS

A. Simple standard cases

To illustrate the application of the concept of symmetry constraint we begin with the consideration of a number of simple standard cases.

With rare exceptions, the DFT calculations reported in the literature are performed under a symmetry constraint. Historically, the first calculations have been performed for the nonmagnetic state of the systems. The magnetic density was assumed to be zero at each point in the space. The study of magnetically ordered systems began with the collinear ferromagnetism of elementary metals, like Fe and Ni, and of the two-sublattice collinear antiferromagnetism of Cr.[15]

It can be easily shown that the regularities characteristic to all three simplest magnetic states correspond to the symmetry constraint and, indeed, must be stable in the calculations. The stability of the zero value of the magnetic moments in the nonmagnetic state is a consequence of the invariance of the KSH with respect to the time reversal. The stability of the equal values and parallel directions of the atomic moments in Fe and Ni are the consequences of the translational symmetry. The stability of the equal values and antiparallel directions of the magnetic moments of two sublattices in Cr are the consequence of the symmetry operation that combines a lattice translation connecting two sublattices and the time reversal. Any disturbance of the characteristic features of these magnetic states leads to the loss of the invariance of the KSH with respect to the corresponding symmetry operation.

B. Atomically disordered relativistic systems

The magnetic structure of atomically disordered systems is a subject of much interest. The study of such systems within the framework of the DFT is connected with severe difficulties that are the consequences of the lack of periodicity. Usually, the collinear magnetic configuration is considered to be one of the possible magnetic ground states of the system. However, according to the symmetry principles formulated in Sec. II, the magnetic structure of relativistic systems with atomic disorder is always noncollinear. Indeed, in the presence of atomic disorder there is no spatial transformation that leaves the atomic positions invariant. Since the spin-orbit coupling connects the atomic and magnetic subsystems, a separate transformation of these subsystems is not allowed. Correspondingly, the system possesses no symmetry operation that can be responsible for the collinearity of the atomic moments. This leads to the noncollinearity of the magnetic structure.

To verify this conclusion the following DFT calculations have been performed. (See Refs. 9 and 3 for details of the calculational scheme.) First, undistorted bcc Fe was considered. In this case the collinear ferromagnetic structure is stable for both relativistic and nonrelativistic calculations (see Sec. III A). At the next stage, a supercell containing eight atoms was constructed and the atoms were shifted from their positions in the bcc lattice by different vectors collected in Table I. These shifts destroy the symmetry operations of the bcc structure that transform the atoms of the supercell into one another. As a result, there is no symmetry operation that can be responsible for the stability of the collinear directions of the magnetic moments of any two atoms in the super cell. Therefore, according to the symmetry analysis of Sec. II each of the eight atomic moments must deviate from the initial direction. These deviations must be different for each of the eight atoms.

The calculations confirmed these predictions. At the beginning all magnetic moments were directed parallel to the z

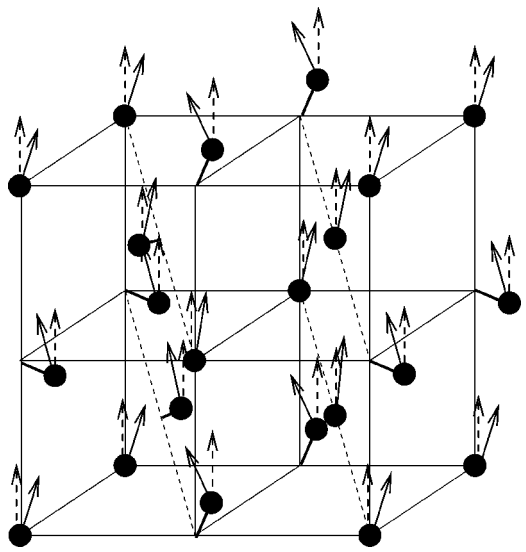

FIG. 2. Atomic disorder leads to the noncollinearity of the magnetic structure. Broken arrows show the initial collinear structure.

axis (Fig. 2). Already the first iteration resulted in different deviations of the moments of all eight atoms from the initial direction. The self-consistent deviation angles are collected in Table I. Important that not only the spin moments of different atoms deviate differently but also the orbital and spin moments of the same atom assume different directions. This property is another consequence of the loss of the symmetry in the system. The collinearity of the spin and orbital moments of the same atom is a regularity that can be stable only if it is supported by a symmetry operation. In the case of symmetry constraint II, the directions of the spin and orbital atomic moments are always different.

Analysis of the calculational process provides an insight into the mechanism of the appearance of the noncollinearity. Crucial quantities are the two-by-two atomic charge matrices, that is the density matrix integrated over atomic spheres. The value of the density matrix depends on the choice of the spin-quantization axis.[16] A convenient choice of the spin-quantization axis of an atom is the direction of the magnetic moment of this atom. The atomic moment will not deviate from the initial direction only in the case that the off-diagonal elements of the integrated density matrix is zero because only in this case the torque on the atomic moment vanishes. Since the off-diagonal element of the matrix is a continuously varying quantity, a symmetry operation must exist that is responsible for the vanishing torque. This is the symmetry operation that is responsible for the stability of the magnetic configuration (see Sec. II).

To study the dependence of the deviations of the magnetic moments on the strength of the spin-orbit coupling and the magnitude of the atomic displacements, two additional calculations have been carried out, one with the SOC and another with the displacements twice the values used in the first calculation (see Table I). We see that there is no simple linear relation between the self-consistent deviation angles, on the one hand, and the SOC and atomic shifts, on the other hand. The absence of a simple linear dependence reflects the complexity of the processes in the system under the influence of the atomic disorder and SOC.

IV. EXCHANGE HELICES IN RELATIVISTIC SYSTEMS

A rich variety of complex magnetic configurations was experimentally found in the heavy rare-earth metals (REM).[17,18] An important contribution to the understanding the magnetic properties of heavy REM is made by Jensen and Mackintosh (see the book[18] and references therein and later publications, e.g., Ref. 19) who used a model spin Hamiltonian to describe peculiar magnetism in these systems. (See also Ref. 20 for earlier phenomenological theory of the magnetic ordering in REM.)

In contrast to the model-Hamiltonian approach, the contribution of the DFT to the study of the complex magnetism in heavy REM is very modest. Most of the DFT calculations for REM were performed for the collinear ferromagnetic structure of Gd. To the best of the author's knowledge, only two direct first-principles DFT calculations of complex magnetic configurations in heavy REM were reported. Nordstöm and Mavromaras[21] used the scalar-relativistic approximation to study the $\mathbf{q}$ dependence of the total energy of planar spiral structures. Here $\mathbf{q}$ is the propagation vector of the spiral. The $E(\mathbf{q})$ curves were compared with the Fourier components of the interatomic exchange parameter $J(\mathbf{q})$ determined experimentally. Perlov *et al.*[22] employed scalar-relativistic approximation to calculate $J(\mathbf{q})$ by examining the conical spiral configurations. No studies of the influence of the SOC on the magnetic configurations of heavy REM have been performed within the framework of the DFT. The success of the DFT in the investigation of the magnetic properties of solids and recent developments in the computational techniques and facilities make the complex magnetism of the heavy REM one of the important topics for the nearest-future studies. Combination of the model-Hamiltonian and first-principles DFT approaches should provide a new level of the theoretical description of REM magnetism.

It is not a purpose of this paper to report a detailed DFT study of the magnetism of concrete REM. Rather we aim to perform the symmetry analysis for a number of magnetic configurations relevant to the REM magnetism, to discuss instabilities connected with the influence of the SOC. All conclusions of the symmetry analysis reported in this section have been verified by the results of first-principles DFT calculations. A contact is made between calculational results and experimental properties.

In the calculations, the $4f$ states were treated as pseudocore[23] states and did not hybridize with the valence-electron states. A scalar-relativistic approximation was used in the description of the core states. The SOC was considered for the valence electrons only. The neglect of the SOC in the $4f$ states is a severe approximation in the physical model describing the effects of the magnetic anisotropy in REM. For example, the SOC in the $4f$ states plays an important role in the description of the magnetic properties of the $4f$ metals in terms of the model crystal-field Hamiltonian.[18] Neglecting the SOC in the $4f$ states we can expect that the

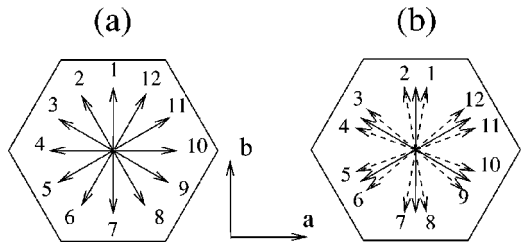

FIG. 3. The 12-layer magnetic configurations in hcp Ho. (a) Planar helical structure. (b) Bunched magnetic structure. Solid arrows: initial structure with pairs of magnetic moments parallel to the crystallographic *b* axes. Broken arrows: the structure obtained under the influence of the SOC (schematic picture).

strength of the magnetic anisotropy will be substantially underestimated. To simulate a stronger magnetic anisotropy within the given calculational scheme in some cases we performed calculations with the SOC enhanced by the factor of 10 or 20.

Several REM were reported to possess a helical magnetic structure. Thus, a planar helix is observed in certain temperature intervals in Tb, Dy, Ho, and Er. A ferromagnetic helix (cone structure) is observed in Ho and Er. The incommensurate helical magnetic structures

$$\mathbf{e}_{\nu}^{\mathbf{q}}=[\sin\theta\cos(\mathbf{qa}_{\nu}+\phi_{\bigcirc})\sin\theta\sin(\mathbf{qa}_{\nu}+\phi_{\bigcirc})\cos\theta] \tag{4.1}$$

although not periodic with the underlying lattice periodicity are very regular. All magnetic moments have equal lengths and their directions are governed by a simple rule: the direction of the moment of an atom at the position $\mathbf{a}_{\nu}$ can be obtained from the direction of the moment at the position $\mathbf{a}_{\mu}$ by the rotation by angle $(\mathbf{a}_{\nu}-\mathbf{a}_{\mu})\mathbf{q}$ about a fixed axis [the *z* axis in the Eq. (4.1)]. According to the consideration of Sec. II, the regularity inherent for helices can be stable property of the system only in the case that there exist symmetry operations responsible for this regularity. In the nonrelativistic case such operation, indeed, exist. These are so-called generalized translations[3] that combine lattice translations $\mathbf{R}_n$ with spin rotations by $\mathbf{qR}_n$ about a fixed axis.

If the SOC is taken into account such operations do not commute with the Hamiltonian of the system and cannot support the regularity characteristic for the helix. Therefore the presence of the SOC must distort the helix.[24] Indeed, a detailed experimental analysis detects the presence of distortions.[18]

We begin the study of the distortions of helices in the relativistic DFT calculations with the consideration of a planar helix with $q=\frac{1}{6}$ [Fig. 3(a)]. This type of commensurate periodicity was observed in Ho. The magnetic moments are parallel to the *ab* plane of the hcp structure. The **q** vector here and in all further examples is parallel to the *c* axis and given in units of $2\pi/c$. The operations describing the symmetry of the KSH in the presence of the SOC are collected in Table II.

The analysis of the transpositions of the atoms under the action of the symmetry operations shows that the atoms can be separated in two groups: {1,3,5,7,9,11} and {2,4,6,8,10,12}. The atoms of the same group are equivalent and the directions of their moments are connected by symmetry transformations. The atoms of different groups are inequivalent and there is no symmetry relation between the directions and lengths of their moments. Analysis of the restrictions on the magnetic moments imposed by the symmetry operations (Table II) shows that all atoms of the first group preserve the initial directions of the magnetic moments [Fig. 3(a)]. For the atoms of the second group the situation is different. Although the directions of the projections of the moments on the *ab* plane must be preserved, the moments can deviate from the *ab* plane without disturbing any of the symmetry operations. Therefore the initial planar structure is unstable. The out-of-plane deviations of moments 2, 6, 10 are equal and opposite to the deviations of moments 4, 8, 12. No ferromagnetic component can appear as a result of these deviations.

An important feature of the experimental magnetic structures in Ho is the effect of bunching. It consists in the deviation of the atomic moments from the uniform distribution [Fig. 3(a)] and grouping of the moments of the atoms of neighboring *ab* planes into pairs with the directions close to one of the crystallographic *b* axes. The symmetry analysis and the results of the DFT calculations show that the effect of bunching cannot be obtained if the calculation begin with the regular helical structure shown in Fig. 3(a).

Next we consider a strongly bunched structure with pairs of neighboring magnetic moments parallel to the *b* axes [Fig. 3(b)]. Although the period of this structure is equal to the period of the helix [Fig. 3(a)], the symmetry of the two structures is different (Table II). This confirms that the bunching cannot be obtained in the calculations that use the helix in Fig. 3(a) as an initial magnetic configuration. Symmetry analysis shows that in the bunched structure all atoms are equivalent. The following distortions of this structure must take place under the influence of the SOC. We begin with the discussion of the in-plane components of the atomic moments. There are two subgroups of the atoms: 1,3,5,7,9,11 and 2,4,6,8,10,12. Within each of the subgroups the moments preserve their initial relative directions: the angles between the moments are proportional to 60°. Both groups of moments rotate as a whole about the *c* axis. The values of the rotation angle are opposite for the groups. Thus the perfect bunching of the initial structure must be replaced by a structure with the moments deviated from the *b* axes [Fig. 3(b)]. The value of this deviation cannot be predicted on the basis of the symmetry arguments and depends on the details of the calculational model. Our calculations gave the value of the deviation angle close to 15° and the resulting magnetic structure close to a uniform helix with angles between atomic moments proportional to 30°. (The experimental deviation is about 6°.[18]) This result shows that the in-plane magnetic anisotropy is underestimated in the calculation.

In addition to the in-plane deviations of the atomic moments, the symmetry analysis predicts the out-of-plane deviations of the moments. The out-of-plane deviations of moments 1, 2, 5, 6, 9, 10 are equal and opposite to the deviations of moments 3, 4, 7, 8, 11, 12. A small out-of-plane deviations of the atomic moments were detected

TABLE II. Generators of the symmetry groups for a number of magnetic states in hcp metals. Number of atoms in the magnetic unit cell n_{at} characterizes the periodicity of the magnetic structure along the c axis. C_{2a}, C_{2b}, and C_{2c} are 180° rotations about the a, b, and c axis, respectively; C_{3c} is a 120° rotations about the c axis; σ_a and σ_c are the reflections in the plane orthogonal to the axis a and c, respectively; I inversion; R time reversal. Vectors in the column "Operation" give the nonprimitive translations entering the symmetry operations. First two components of the translation are given in a units, the third component in c units. Atoms not presented in the column "Transposition" are invariant with respect to the given symmetry operation.

Magnetic structure	n_{at}	Operation	Transposition	Restriction on magnetic moments [a]
Helix, ab plane	12	C_{2b}	$2\leftrightarrow12;3\leftrightarrow11;4\leftrightarrow10;$ $5\leftrightarrow9;6\leftrightarrow8;$	Type C_{2b}
[Fig. 3(a)]		$C_{3c}(0,0,2)$	$1\rightarrow5\rightarrow9\rightarrow1;2\rightarrow6\rightarrow10\rightarrow2;$ $3\rightarrow7\rightarrow11\rightarrow3;4\rightarrow8\rightarrow12\rightarrow4;$	Type C_{3c}
		$R(0,0,3)$	$1\leftrightarrow7;2\leftrightarrow8;3\leftrightarrow9;$ $4\leftrightarrow10;5\leftrightarrow11;6\leftrightarrow12;$	Type R
Bunched	12	$C_{2a}\left(0,\frac{\sqrt{3}}{3},\frac{7}{2}\right)$	$1\leftrightarrow8;2\leftrightarrow7;3\leftrightarrow6;$	Type C_{2a}
[Fig. 3(b)]			$4\leftrightarrow5;9\leftrightarrow12;10\leftrightarrow11;$	
		$C_{3c}(0,0,2)$	$1\rightarrow5\rightarrow9\rightarrow1;2\rightarrow6\rightarrow10\rightarrow2;$ $3\rightarrow7\rightarrow11\rightarrow3;4\rightarrow8\rightarrow12\rightarrow4;$	Type C_{3c}
		$R(0,0,3)$	$1\leftrightarrow7;2\leftrightarrow8;3\leftrightarrow9;$ $4\leftrightarrow10;5\leftrightarrow11;6\leftrightarrow12;$	Type R
Helix, ab plane	8	C_{2b}	$2\leftrightarrow8;3\leftrightarrow7;4\leftrightarrow6;$	Type C_{2b}
[Fig. 4(a)]		$R(0,0,2)$	$1\leftrightarrow5;2\leftrightarrow6;3\leftrightarrow7;4\leftrightarrow8;$	Type R
Cycloid, bc-plane	8	C_{2b}	$2\leftrightarrow8;3\leftrightarrow7;4\leftrightarrow6;$	Type C_{2b}
[Fig. 4(b)]		$\sigma_a(0,0,2)$	$1\leftrightarrow5;2\leftrightarrow6;3\leftrightarrow7;4\leftrightarrow8;$	Type C_{2a}
		$R(0,0,2)$	$1\leftrightarrow5;2\leftrightarrow6;3\leftrightarrow7;4\leftrightarrow8;$	Type R
Cycloid, ac plane	8	$\sigma_c(0,0,2)$	$1\leftrightarrow5;2\leftrightarrow4;6\leftrightarrow8;$	Type C_{2c}
		$R(0,0,2)$	$1\leftrightarrow5;2\leftrightarrow6;3\leftrightarrow7;4\leftrightarrow8;$	Type R
Helix, ab plane	14	$C_{2c}\left(0,\frac{\sqrt{3}}{3},\frac{7}{2}\right)$	$1\leftrightarrow8;2\leftrightarrow9;3\leftrightarrow10;4\leftrightarrow11;$	Type C_{2c}
[Fig. 5(a)]			$5\leftrightarrow12;6\leftrightarrow13;7\leftrightarrow14;$	
		RC_{2b}	$2\leftrightarrow14;3\leftrightarrow13;4\leftrightarrow12;$ $5\leftrightarrow11;6\leftrightarrow10;7\leftrightarrow9;$	Type σ_b

[a]Type E: $\mathbf{m}_j=\mathbf{m}_i$; type C_{2a}: $\begin{pmatrix} m_a \\ m_b \\ m_c \end{pmatrix}_j = \begin{pmatrix} m_a \\ -m_b \\ -m_c \end{pmatrix}_i$; type C_{2b}: $\begin{pmatrix} m_a \\ m_b \\ m_c \end{pmatrix}_j = \begin{pmatrix} -m_a \\ m_b \\ -m_c \end{pmatrix}_i$; type C_{2c}: $\begin{pmatrix} m_a \\ m_b \\ m_c \end{pmatrix}_j = \begin{pmatrix} -m_a \\ -m_b \\ m_c \end{pmatrix}_i$;

type C_{3c}: $\begin{pmatrix} m_a \\ m_b \\ m_c \end{pmatrix}_j = \begin{pmatrix} -\frac{1}{2}m_a-\frac{\sqrt{3}}{2}m_b \\ \frac{\sqrt{3}}{2}m_a-\frac{1}{2}m_b \\ m_c \end{pmatrix}_i$; type R: $\mathbf{m}_j=-\mathbf{m}_i$; type σ_b: $\begin{pmatrix} m_a \\ m_b \\ m_c \end{pmatrix}_j = \begin{pmatrix} m_a \\ -m_b \\ m_c \end{pmatrix}_i$.

Here i and j are according to the column "Transposition." Atom i is transformed to atom j under the action of the symmetry operation. For atoms invariant under the action of the symmetry operation, $j=i$.

experimentally.[25] Note that a model spin Hamiltonian that contains only the terms of the second order with respect to atomic spins: the Heisenberg exchange interaction and the single-site magnetic anisotropy, fails to describe these deviations. The forth-order "trigonal" interactions must be added.[19] In the magnetic and relativistic DFT calculations these and higher order interactions are automatically taken into account. Test calculations for Ho gave small out-of-plane deviations that do not exceed a few tenths of a degree, also in the case the SOC is enhanced by a factor of 10. This deviation is smaller than the experimental value of about 2°.[25]

In the case of Er the structures with $q=\frac{1}{4}$ are of interest.[18] First, we consider the influence of the SOC on a planar helix with $q=\frac{1}{4}$ [Fig. 4(a)] The generators of the symmetry group are given in Table II. There are three groups of equivalent atoms: {1,5}, {3,7}, {2,4,6,8}. The moments of atoms 1 and 5 must keep their initial directions parallel to the b axis.

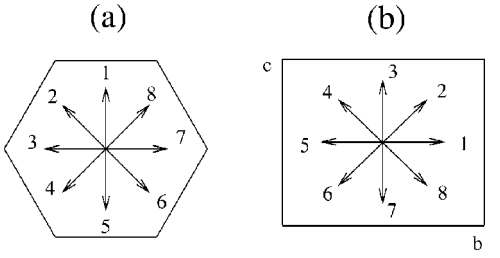

FIG. 4. The 8-layer magnetic configurations in hcp Er. (a) The initial planar helical structure. All moments are parallel to the ab plane. (b) The calculated planar magnetic structure. All moments are parallel to the bc plane.

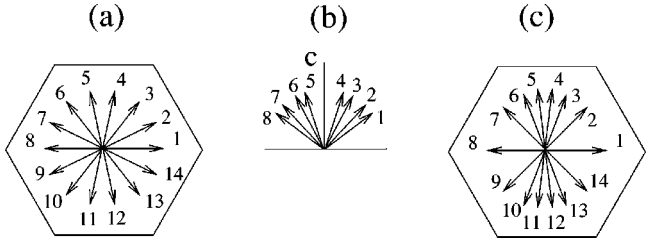

FIG. 5. The 14-layer magnetic configurations in hcp crystal structure. (a) The initial planar helical structure. All moments are parallel to the ab plane. (b) The deviation of the magnetic moments from the ab plane under the influence of the SOC (schematic picture). (c) The in-plane configuration of the magnetic moments distorted by the SOC (schematic picture).

Atomic moments 3 and 7 deviate within the ac plane, no b component can appear. Moments 2,4,6,8 move both within the ab plane and out of the ab plane. No ferromagnetic component can appear.

Numerical calculations started with this helical structure gave an interesting result that differs drastically with the results obtained in the calculations for Ho. For the SOC scaled by a factor of 20 the moments deviate strongly from the ab plane and result in the magnetic configuration shown in Fig. 4(b). Thus, the initial planar magnetic configuration with moments parallel to the horizontal ab plane is replaced by a planar magnetic structure parallel to the vertical bc plane. This transformation of the magnetic configuration is not forbidden by symmetry since all the symmetry elements of the initial structure are preserved. The final magnetic state is more symmetrical than the initial one since the symmetry group contains one additional generator (Table II). This example illustrates the property that the symmetry of the state of the system can increase in the calculations.

The difference in the behavior of the helical structures in Ho and Er reflects difference in the character of the magnetocrystalline anisotropy that is in agreement with the experimental data.[18] The planar vertical structure obtained in the calculations is in good agreement with a vertical planar cycloidal structure found experimentally in Er. Two structures are, however, not identical: The calculations resulted in a structure parallel to the bc plane. The experimental structure is parallel to the ac plane. A wobbling of the vertical structure found experimentally is also not reproduced in this calculation. The reason for this disagreement is, again, connected with the symmetry of the initial state. Indeed, the structure shown in Fig. 4(a) cannot transform within the DFT calculations into the planar structure parallel to the ac plane since this transformation leads to a loss of symmetry operations.

To understand the nature of the wobbling of the experimental vertical structure we performed the symmetry analysis for a magnetic configuration shown in Fig. 4(b) but, in this case, parallel to the ac plane. The symmetry of this structure preserves (i) the directions of the atomic moments 3 and 7, (ii) the zero c component of the moments 1 and 5, and (iii) the compensated character of the structure as a whole. Moments 2–4 and 6–8 deviate from the ac plane leading to the wobbling observed experimentally. Similar to the out-of-plane deviations of the atomic moments in the $q=\frac{1}{6}$ structure of Ho, the forth-order trigonal terms must be added to the model Hamiltonian to describe the wobbling.[19] No further terms need to be included into the magnetic and relativistic KSH to describe this effect.

To study the dependence of the properties of the magnetic structure on the propagation vector we considered a planar helical structure with atomic moments parallel to the ab plane and $q=\frac{1}{7}$ [Fig. 5(a)]. The symmetry operations are collected in Table II. There are four groups of equivalent atoms: {1,8}, {2,7,9,14}, {3,6,10,13}, {4,5,11,12}. The b component of moments 1 and 8 must be zero. For any of the four groups, the in-plane components of the moments compensate. Remarkable, however, that there is no symmetry restriction demanding the compensation of the c components of the atomic moments. Therefore the initial planar magnetic structure [Fig. 5(a)] breaks, in the presence of the SOC, the equivalence of the positive and negative directions of the c axis that inevitably leads to the formation of a ferromagnetic component along the c axis. This example shows that the distortion of the in-plane helix by the SOC is, under certain conditions, connected with the appearance of a ferromagnetic component along the c axis. Figures 5(b) and 5(c) show schematically the distorted magnetic structure.

V. CONCLUSIONS

We used the notion of symmetry constraint to discuss the stability of the regular features of a magnetic structure in the DFT calculations and in nature. On the basis of symmetry arguments and first-principles DFT calculations we show that the magnetic structure of a relativistic system with atomic disorder is always noncollinear.

We report the symmetry analysis and illustrative first-principles DFT calculations for a series of magnetic configurations relevant to the magnetism of REM. Correlations between the numerical results and experimental data are obtained. Restrictions of the present calculational scheme do not allow direct quantitative comparison of the calculational results for REM with experiment. Since the magnetic anisotropy is very sensitive to the details of the theoretical model, future systematic DFT studies of the REM magnetism should consider such effects as polar magnetic interaction of atomic moments and lattice distortion caused by magnetoelastic interactions.[20] The account for the SOC in the $4f$ states is of

great importance. Another important direction for the improvement of the calculational scheme is a better account for the correlation effects in the $4f$ states. Here self-interaction corrections,[26] orbital polarization corrections[27] or local density approximation (LDA)$+U$ (Ref. 28) scheme should be considered as possible approaches. Combination of these improvements should make possible a first-principles quantitative description of the delicate balance of different interactions traditionally described in terms of a model crystal-field Hamiltonian.[18] Detailed DFT study of the magnetism of heavy REM with account for the SOC and noncollinearity of the magnetic structure is an exciting topic for the nearest-future researches. The symmetry analysis reported here preserves its validity also for more elaborated physical models. We hope that the present symmetry analysis and results of numerical calculations will stimulate further studies of the complex magnetism in REM systems.

ACKNOWLEDGMENT

The comments of Jens Jensen on the REM part of the manuscript were very important and are gratefully acknowledged.

[1] L. D. Landau and E. M. Lifshitz, *Statistical Physics* (Pergamon, New York, 1980), Part 1.

[2] J.-C. Tolédano and P. Tolédano, *The Landau Theory of Phase Transitions* (World Scientific, Singapore, 1987).

[3] L. M. Sandratskii, Adv. Phys. **47**, 91 (1998).

[4] L. M. Sandratskii and J. Kübler, Phys. Rev. Lett. **75**, 946 (1995).

[5] L. M. Sandratskii and J. Kübler, Phys. Rev. B **60**, R6961 (1999).

[6] L. M. Sandratskii and G. Lander, Phys. Rev. B **63**, 134436 (2001).

[7] D. H. Lyons and T. A. Kaplan, Phys. Rev. **120**, 1580 (1960).

[8] The approximations are often the consequences of the complexity of the calculational problem and are made to make the problem tractable.

[9] L. M. Sandratskii and J. Kübler, Phys. Rev. B **55**, 11395 (1997).

[10] P. H. Dederichs, S. Blügel, R. Zeller, and H. Akai, Phys. Rev. Lett. **53**, 2512 (1984).

[11] B. L. Györffy, A. J. Pindor, J. Staunton, G. M. Stocks, and H. Winter, J. Phys. F: Met. Phys. **15**, 1337 (1985).

[12] The property that the state providing the minimum of the functional under the symmetry restrictions does not need a stabilizing field can also be proved in a more general form, without referring to the Kohn-Sham minimization procedure. It can be shown that the energy functional has a zero-variational derivative at the density that supplies the minimum of the energy functional under the constraining symmetry conditions. Gunarsson and Lundqvist [O. Gunarsson and B. I. Lundqvist, Phys. Rev. B **13**, 4274 (1976)] considered the case of a Hamiltonian commuting with the operator of an observable and discussed the minimization of the total energy functional for different eigenvalues λ of the observable. They have shown that in this case the constrained minimization of a universal functional is replaced by an unconstrained minimization of a λ-dependent functional that is carried out separately for each λ.

[13] K. Knöpfle, L. M. Sandratskii, and J. Kübler, Phys. Rev. B **62**, 5564 (2000).

[14] K. Knöpfle and L. M. Sandratskii, Phys. Rev. B **63**, 014411 (2001).

[15] Deviation of the propagation vector of the magnetic structure of Cr from 0.5 was not taken into account in early calculations.

[16] J. Sticht, K. H. Höck, and J. Kübler, J. Phys.: Condens. Matter **1**, 8155 (1989).

[17] W. C. Koehler, in *Magnetic Properties of Rare Earth Metals*, edited by R. J. Elliott (Plenum Press, London, 1972), p. 81.

[18] J. Jensen and A. R. Mackintosh, *Rare Earth Magnetism* (Clarendon Press, Oxford, 1991).

[19] J. Jensen, Acta Phys. Pol. A **91**, 89 (1997).

[20] B. R. Cooper, in *Magnetic Properties of Rare Earth Metals*, (Ref. 17), p. 17.

[21] L. Nordström and A. Mavromaras, Europhys. Lett. **49**, 775 (2000).

[22] A. Y. Perlov, S. V. Halilov, and H. Eschrig, Phys. Rev. B **61**, 4070 (2000).

[23] M. S. S. Brooks, L. Nordström, and B. Johansson, J. Phys.: Condens. Matter **3**, 2357 (1991); M. Richter and H. Eschrig, Physica B **172**, 85 (1991).

[24] In this respect, the results of the early paper by Lyons and Kaplan are worth noting (Ref. 7). The authors have shown that the ground state of the system of equivalent classical Heisenberg spins is always a helix. Since the classical Heisenberg exchange energy is invariant with respect to generalized translations this result is in agreement with our arguments. Although Lyons and Kaplan did not refer directly to the generalized translations, they emphasized the relation between the symmetry of the energy expression and the helical ground state. An important difference between the present discussion and the discussion in Ref. 7 is in the treatment of collinear magnetic states. Whereas the conclusions of Lyons and Kaplan are valid in the case the collinear ferromagnetism and collinear antiferromagnetism are considered as particular cases of helices, our statements are made for *incommensurate* helical structures. In contrast to incommensurate helices, the collinear magnetic structures can be stable in the relativistic case.

[25] R. A. Cowley and S. Bates, J. Phys. C **21**, 4113 (1988).

[26] P. Strange, A. Svane, W. M. Temmerman, Z. Szotek, and H. Winter, Nature (London) **399**, 756 (1999).

[27] O. Eriksson, B. Johansson, and M. S. S. Brooks, J. Phys.: Condens. Matter **1**, 4005 (1989).

[28] V. Anisimov, J. Zaanen, and O. K. Andersen, Phys. Rev. B **44**, 943 (1991); A. I. Liechtenstein, V. P. Antropow, and B. N. Harmon, *ibid.* **49**, 10 770 (1994).